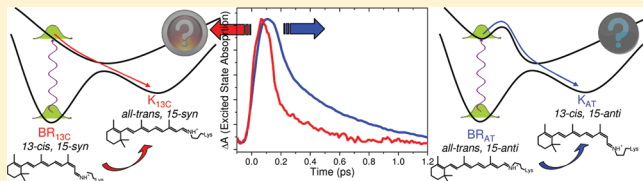


# Ultrafast Photochemistry of Light-Adapted and Dark-Adapted Bacteriorhodopsin: Effects of the Initial Retinal Configuration

Amir Wand,<sup>†</sup> Noga Friedman,<sup>‡</sup> Mordechai Sheves,<sup>‡</sup> and Sanford Ruhman\*,<sup>†</sup><sup>†</sup>Institute of Chemistry and the Farkash Center for Light-Induced Processes, The Hebrew University of Jerusalem, Edmond J. Safra Campus, Givat Ram, Jerusalem 91904, Israel<sup>‡</sup>Department of Organic Chemistry, The Weizmann Institute of Science, Rehovot 76100, Israel

**ABSTRACT:** Femtosecond spectroscopy is used to compare photochemical dynamics in light-adapted and dark-adapted bacteriorhodopsin (BR). The retinal prosthetic group is initially all-trans in the former, while it is nearly a 1:1 mixture with 13-cis in the latter. Comparing photochemistry in both serves to assess how the initial retinal configuration influences internal conversion and photoisomerization dynamics. Contrary to an earlier study, our results show that after excitation of the 13-cis form it crosses back to the ground state much more rapidly than the biologically active all-trans reactant. A similar result was recently obtained for another microbial retinal protein, Anabaena Sensory Rhodospin (ASR), which can be toggled by light between two analogous ground state configurations. Together, these studies suggest that this disparity in rates may be a general trend in the photochemistry of microbial retinal proteins. This may bear as well on the well-known enhancement in photoisomerization rates going from microbial retinal proteins to the visual pigments, as the latter also start the course of photoreception in a cis retinal configuration, in that case 11-cis. In lieu of indications for pretwisting or straining of the 13-cis retinal forms of BR and ASR, akin to those reported for rhodopsin, current results challenge many of the mechanisms held responsible for the ballistic photochemical dynamics observed in visual pigment.



Primary steps of the  $\text{BR}_{\text{AT}}$  photocycle, from photoabsorption to the formation of the isomerized photoproduct K, have been extensively studied.<sup>8–17</sup> The subpicosecond reactive excited state coined “ $I_{460}$ ”, the fluorescent state, exhibits a transient difference spectrum which, aside from an induced bleach of the reactant absorption band at 570 nm, consists of near-IR (NIR) overlapping absorption and stimulated emission bands producing a peak emission at  $\sim 850$  nm and an additional “blue” absorption band centered near  $\sim 500$  nm.

The initial buildup of the  $I_{460}$  fluorescent state, heavily involving a rapid reorganization of carbon–carbon bond lengths,<sup>18–24</sup> is manifested by an initial  $\sim 100$  fs phase of spectral evolution.<sup>13,17,25,26</sup> The later decay to form ground state “ $J_{625}$ ” and then “ $K_{590}$ ” intermediates is markedly nonexponential and is accompanied by mild spectral evolution of the difference spectrum described above.<sup>9,10,25,27</sup> Understanding the molecular dynamics underlying these changes is still ongoing. Fitting the transient spectra leading up to  $J$  with a kinetic model requires the inclusion of a number of formal intermediates, even excluding the initial shifts involved in establishing the fluorescent state. Nonetheless, most researchers doubt that this reflects distinct intermediate states, viewing it likely that this reflects residual excited state cooling or structural

## INTRODUCTION

Bacteriorhodopsin (BR), a trans-membrane protein, acts as a light-driven proton pump in the archaeon *Halobacterium salinarum*.<sup>1</sup> The chromophore in BR is a retinal, covalently bound to a lysine residue on the seventh helix via a protonated Schiff base linkage (RPSB). In the dark, slow thermal isomerization at room temperature leads, at equilibrium, to the so-called dark-adapted form of BR (DA-BR), which consists of an almost even mixture of two ground state forms: one with the retinal all-trans, 15-anti ( $\text{BR}_{\text{AT}}$ ), and the other 13-cis, 15-syn ( $\text{BR}_{13\text{C}}$ ). Moderate irradiation in the visible changes this to light-adapted BR (LA-BR), which is almost pure  $\text{BR}_{\text{AT}}$ .<sup>2,3</sup>

Absorption of light by  $\text{BR}_{\text{AT}}$  initiates a photocycle, starting with specific isomerization around the  $\text{C}_{13}=\text{C}_{14}$  double bond leading to the so-called “J” photointermediate, cooling within a few picoseconds to “K”. The cycle continues through a set of distinct spectroscopic intermediates (L, M, N, and O), leading back to the initial state in  $\sim 15$  ms after ejecting a single proton through the cell membrane. Much less is known about the photocycle of  $\text{BR}_{13\text{C}}$ . Nanosecond time-resolved studies reported a  $\sim 40$  ms lifetime intermediate absorbing at  $\sim 610$  nm (“ $K_{610}$ ”),<sup>4–6</sup> assigned by FTIR to be in an all-trans, 15-syn configuration.<sup>7</sup>  $K_{610}$  thermally decays mainly back to  $\text{BR}_{13\text{C}}$  but also to a lesser degree to  $\text{BR}_{\text{AT}}$ . Continuous illumination, however, produces  $\sim 100\%$  pure  $\text{BR}_{\text{AT}}$  in the so-called ‘light-adaptation’ process since the  $\text{BR}_{\text{AT}}$  photocycle exclusively repopulates the all-trans reactant state.

**Special Issue:** Richard A. Mathies Festschrift

**Received:** December 28, 2011

**Revised:** February 6, 2012

**Published:** February 13, 2012

evolution, in a system whose size and flexibility should already exclude homogeneous exponential kinetics. This picture was upheld in three pulse (pump–dump–probe) experiments conducted in our lab, demonstrating a constant cross section for emission throughout the fluorescent state lifetime.<sup>25</sup> A similar conclusion was also obtained in similar experiments conducted more recently on the analogous process in *pharaonis* Halorhodopsin.<sup>28</sup>

The mild spectral evolution of I<sub>460</sub> over the course of internal conversion (IC) to J and the reported steadiness in the cross section for stimulated emission from the fluorescent state are inconsistent with a “ballistic” IC in the form of a compact nuclear wave packet concertedly crossing to the ground state. This, however, is the picture arising from ultrafast spectroscopic study of the primary events in vision, where dramatic spectral evolution continues throughout the much faster process of IC.<sup>11,29–31</sup> It is interpreted to reflect constant variation of emission and absorption resonance frequencies as the reactive wavepacket evolves. Localization of this wavepacket is shown even to survive the act of curve crossing, as exhibited by the resulting periodical spectral modulations in pump–probe signals of the nascent photo/batho-rhodopsin, photointermediates of the visual pigment.<sup>31</sup> These aspects have recently been vividly demonstrated using broadband hyperspectral coverage of this process with sub-20 fs resolution.<sup>32</sup>

Understanding why the photochemical dynamics of the two branches of the retinal protein (RP) family differ so has occupied photobiologists for decades. Structural investigations of the 11-*cis* retinal chromophore in its surroundings in the visual pigment rhodopsin (RH) show that inclusion in the protein breaks the planar symmetry of the polyene chain,<sup>33–36</sup> suggested by theoretical modeling to determine the initial direction of twisting and facilitating the direct unhindered transition to the ground state.<sup>37–42</sup> Comparable studies of BR indicate no such pretwisting and crowding of the retinal,<sup>35,43,44</sup> and this difference between the two proteins is borne out by analysis of their resonance Raman spectra. The factors determining the divergence in dynamics of BR and RH photochemistry must, however, involve details of the retinal conformation and of retinal–protein interactions, given the structure of the protein pocket and the positioning of polarizable and charged protein residues.

One way to separate the underlying mechanisms would be to induce controlled changes within a single protein, either in the prosthetic group or its protein surroundings, and follow how they influence the dynamics of IC and isomerization. A comparative study of photochemistry in RH and in isorhodopsin (iso-RH) was conducted in this spirit.<sup>31,45,46</sup> Shifting the initial RPSB configuration from 11-*cis* to 9-*cis*, with no changes in the protein itself, was shown to significantly enhance the excited state lifetime, producing the same product bathorhodopsin with much lower probability. This was interpreted as stressing the bond specificity in protein catalysis of IC in RH, presumably due to steric interaction of the C<sub>13</sub> methyl group which is specific to the 11-*cis* configuration. Recent experiments with improved time resolution show, however, that a major component of IC in iso-RH still takes place within ~200 fs, suggesting that the course of reaction in both systems may be more similar than initially thought.<sup>47</sup> In any case, the assumption that bond isomerization is the limiting step for curve crossing in RH has recently been challenged by Mathies and co-workers, who maintain that aside from C=C bond order alternation rearrangement, IC of ca. 50 fs is

facilitated mainly by hydrogen out-of-plane (HOOP) vibrations (with a period of ~36 fs), weakening the case for the suggested mechanism for the change in the observed rates between RH and iso-RH.<sup>48,49</sup> These experimental results are further supported by theoretical works, which show that the phase and amplitude of HOOP modes associated with the involved double bond determine the rate and quantum efficiencies of photoisomerizations between RH and bathorhodopsin.<sup>40,50</sup>

In BR, “locking” of the active C<sub>13</sub>=C<sub>14</sub> double bond by inclusion in an aliphatic ring was shown to prolong the fluorescent state lifetime by nearly 2 orders of magnitude,<sup>16,51</sup> an effect which was not observed in equivalent experiments on the RPSB in solution, showing again a mode specificity of RPSB chemistry within the opsin surroundings. Furthermore, specific mutations to the opsin, as well as deionizing BR to transform “purple” to “blue” membranes, have been shown in femtosecond pump–probe experiments to develop new picosecond IC components.<sup>26,52–55</sup> While these have been assigned to a ground state mixture of all-*trans* and 13-*cis* configurations, the results are contradictory, with the relative efficiency of protein catalysis in these two varying widely and no general arising trend observed.

Alternatively, this question can be addressed by comparing photoisomerization dynamics in light-adapted and dark-adapted BR. As described above, dark adaptation overnight at room temperature naturally results in a fairly even mixture of BR<sub>AT</sub> and BR<sub>13C</sub>, without any tampering with protein structure or physiological conditions. A pioneering comparative study of LA-BR and DA-BR, aimed at testing the effect of changing the initial retinal configuration on primary events in BR, was conducted nearly three decades ago by Petrich et al.<sup>8</sup> Remarkably, no significant change in IC kinetics was recorded in those experiments. Technological limitations at the time restricted the sensitivity of those experiments to contributions from the BR<sub>13C</sub> reactants. Nonetheless, the conclusion drawn was that both ground state configurations react to absorption of light with similar rates, already characterized earlier for BR<sub>AT</sub>.

A recent study from our laboratories<sup>56</sup> has rekindled our interest in the comparison conducted by Petrich et al. In it, the excited state dynamics of the Anabaena Sensory Rhodopsin (ASR), another microbial retinal protein (MRP) found in the fresh-water cyanobacterium *Anabaena* (*Nostoc*) sp. PCC 7120, was investigated<sup>57</sup> (see ref 58 and the references therein). Unlike BR, ASR functions not as an ion pump but as a photoswitch, toggling by absorption between two stable ground state configurations. In analogy with BR, these are again 13-*cis*,15-*syn* (ASR<sub>13C</sub>) and all-*trans*,15-*anti* (ASR<sub>AT</sub>). Unlike BR, dark adaptation leads to ~100% ASR<sub>AT</sub> while continuous irradiation in the visible produces a mixture at ratios which vary with irradiation wavelength. This has prompted the suggestion that ASR is a sensory photoreceptor which activates chromatic adaptation in the host bacterium. Our comparison of primary events in light- and dark-adapted ASR shows a drastic asymmetry in the excited state lifetimes, with IC rates starting with ASR<sub>13C</sub> being about 10-fold faster than when starting with ASR<sub>AT</sub>. This result differs with respect to the effect of retinal configuration from that obtained for BR, raising the possibility that the experimental limitations commented on by the authors might have led to erroneous conclusions.

To determine this, we have performed a new comparison of primary light-induced processes in light- and dark-adapted samples of BR, using tunable femtosecond pump–broadband hyperspectral probe methods. Extraction of the underlying

$\text{BR}_{\text{AT}}$  (directly from LA-BR) and  $\text{BR}_{13\text{C}}$  photodynamics shows that, as in the case of the ASR, *cis* to *trans* isomerization is much faster than for  $\text{BR}_{\text{AT}}$  and reminiscent of the ballistic dynamics of the visual pigments. Along with previous results obtained with ASR,<sup>56</sup> and some of the experiments with deionized BR and BR mutants,<sup>26,52,53</sup> this suggests that *cis* to *trans* photoisomerization in MRPs is much faster than in the opposite direction, prompting revision of our understanding of protein catalysis of photoisomerization in RPs in general and of photochemical differences between type-1 and type-2 rhodopsins in particular.

## EXPERIMENTAL SECTION

**Sample Preparation and Handling.** *Halobacterium salinarum* was grown from the S9 strain, and purple membranes containing bacteriorhodopsin were isolated as previously described.<sup>59</sup> Potassium phosphate buffer was used to maintain a neutral pH. Room temperature samples with nominal OD of ~0.5 at 570 nm were syringe pumped through a ~0.4 mm path length cell, equipped with 0.2 mm fused silica windows. Sample integrity was determined spectrophotometrically before and after the runs. DA-BR samples were kept in the dark overnight at room temperature and protected from photoconversion during experimental runs by eliminating photochemically effective ambient light. Photoconversion of DA-BR was verified to be  $\leq 10\%$  by spectrophotometry under experimental conditions. LA-BR was prepared by irradiation with white light from a 150 W quartz halogen fiber bundle light source for ~15 min prior to the experiment, and the sample was continuously light adapted during pump–probe measurements.

**Pump–Probe Experiments.** The laser system and pump–probe setup are similar to those used in the recent study of the ASR protein.<sup>56</sup> Briefly, a home-built multipass amplified titanium sapphire apparatus, producing an 800 Hz train of 0.5 mJ pulses centered at 800 nm (fwhm ~40 nm, ~30 fs), was used as the seed for pump and probe pulses. Pump pulses of ~25 fs duration and centered at 560 nm (see Figure 1) were obtained from a TOPAS optical parametric amplifier (Light Conversion). Broadband supercontinuum pulses were generated by focusing ~1  $\mu\text{J}$  of the fundamental in 1.5 mm of sapphire and were split into probe and reference beams. The

former was collimated and refocused into the sample with reflective optics. A 40–50 nJ pump beam was focused to a spot 200  $\mu\text{m}$  in diameter and overlapped with the probe which was nearly two times smaller.

The probe and reference pulses were directed through fibers to a double diode array spectrograph setup to generate time-dependent absorption spectra in the ~450–850 nm spectral region. Such absorption spectra were taken with and without pump, and subtraction of these provided wavelength-dependent optical density difference spectra ( $\Delta\text{OD}(\lambda,t)$ ). Signal amplitudes were demonstrated to be linear in pump intensity up to 2 times that used in experiments. Dispersion of pump pulses was compensated for in a slightly misaligned zero-dispersion grating pulse shaper and that of the probe by standard methods of time correction based on experimentally determined group delay dispersion, leading in total to a nominal temporal resolution of ~70–90 fs.<sup>60</sup>

**Isomeric Composition of the Samples.** On the basis of steady state absorption spectra of the two isomers of BR,<sup>6</sup> the isomeric compositions of our DA-BR and LA-BR were fit to ~50:50% 13-*cis*/all-*trans* and >95% all-*trans* mixtures, respectively, as demonstrated in Figure 1. This is in accordance with previous studies, which determined the 13-*cis*/all-*trans* ratio in the former to be in the range of 1 to 1.5.<sup>2,3</sup> Accordingly, throughout this study, we assume that the LA-BR sample is pure  $\text{BR}_{\text{AT}}$ , and the DA-BR is a 50–50% mixture.

## RESULTS

**Ultrafast Pump–Probe Data.** Color-coded contour maps of transient changes in optical density as a function of time and probe wavelength ( $\Delta\text{OD}(\lambda,t)$ ) are shown in Figure 2 for LA-BR (left) and DA-BR (middle). The general appearance of both samples is similar, demonstrating the spectral features described above in the Introduction and previously reported for light-adapted samples. These include a rapid buildup of excited state absorption and emission to the blue and to the red of the ~570 nm ground state bleach, respectively, early spectral shifting, and gradual decay of these features within a few picoseconds, leaving behind the signature of the red-shifted ground state product K, again apparent in both samples. The main difference between the two is an apparent shortening of the excited state lifetime in the case of DA-BR relative to the LA-BR. The right panel presents the contribution of the 13-*cis* initial population to the DA-BR data, itself depicted in the middle. The methods of its isolation will be addressed shortly below. Spectral cuts in the same three data sets are shown in Figure 3 for four representative probing wavelengths, clearly demonstrating that the photodynamics in  $\text{BR}_{13\text{C}}$  are much faster than in  $\text{BR}_{\text{AT}}$ .

Assuming independent contributions from both isomeric forms to the transient spectra of excited DA-BR, isolating that from  $\text{BR}_{13\text{C}}$  requires the subtraction of a properly weighted replica of LA-BR data from pump–probe results obtained from samples kept in the dark. Determining the correct subtraction factor is nontrivial, as it involves not only the relative abundance of the two configurations in DA-BR but also their different absorbance, the pump pulse spectrum, and additional experimental factors. As in the study of ASR, we opt to obtain this ratio empirically through a comparison of LA- and DA-BR pump–probe data at later delays. Assuming the independence of contributions listed above, if photoisomerization is significantly faster in  $\text{BR}_{13\text{C}}$ , as the data indeed indicate, at some point of time following excitation the remainder of excited molecules will be exclusively  $\text{BR}_{\text{AT}}^*$ , whether we start

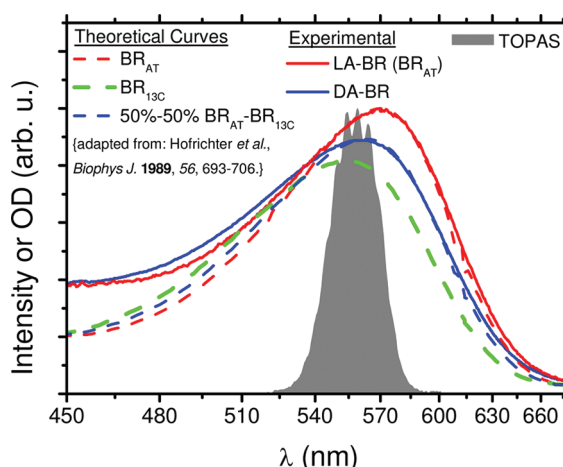


**Figure 1.** Experimental steady state absorption of DA-BR and LA-BR, shown along calculated curves of  $\text{BR}_{\text{AT}}$ ,  $\text{BR}_{13\text{C}}$  (ref 6), and a 50%-50% mix of  $\text{BR}_{\text{AT}}:\text{BR}_{13\text{C}}$ . The latter corresponds well with the experimental DA-BR spectrum. A typical TOPAS excitation spectrum is shown as well.

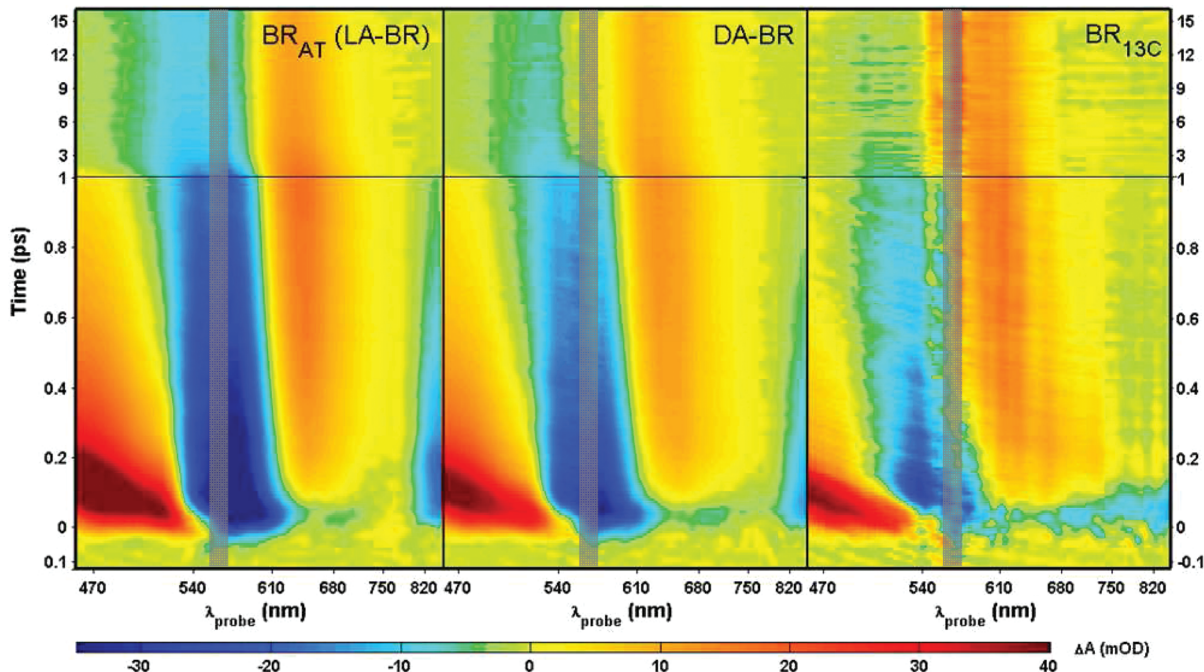


**Figure 2.** Hyperspectral pump–probe data for LA-BR ( $\text{BR}_{\text{AT}}$ ), DA-BR, and  $\text{BR}_{13\text{C}}$ .  $\Delta\text{OD}$  is color coded according to scale below, and the gray-shaded area designates a range where pump scatter limits data reliability. The  $\text{BR}_{13\text{C}}$  is obtained by properly weighted subtraction of LA-BR from DA-BR results and rescaling to represent the pump–probe signal projected to be obtained from the 100%  $\text{BR}_{13\text{C}}$  sample under identical conditions (see text for details).

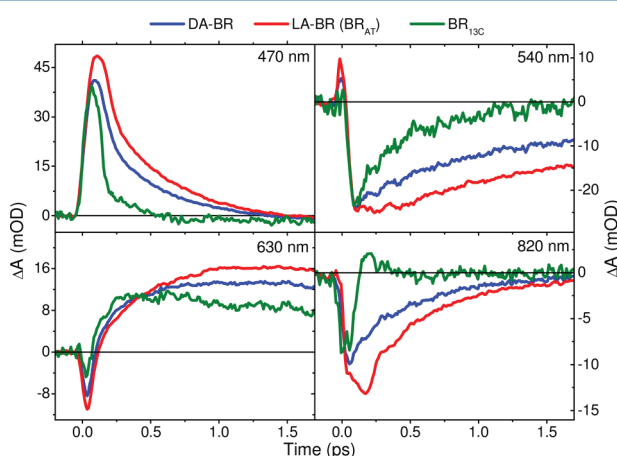


**Figure 3.** Spectral cuts at four representative probing wavelengths of the transient difference spectra of DA-BR (blue), LA-BR (red), and  $\text{BR}_{13\text{C}}$  (green), taken as vertical cuts of the full data in Figure 2. The former two are presented to scale, and the latter was derived from them and rescaled as described in the text and in the caption of Figure 2.

with LA-BR or DA-BR. Accordingly, the dynamic changes in absorption (to be distinguished from the transient spectra themselves, which carry over the signs of any photoproduct formed) should, to within a constant factor, be identical in both experiments. This is demonstrated in Figure 4, which depicts four representative dynamic difference spectra [ $\Delta\text{OD}(t + \delta t) - \Delta\text{OD}(t)$ ] obtained from both data sets. It shows that for delays beyond  $t \sim 0.5$  ps these spectra overlap almost perfectly once scaled by a single factor.

Another way of testing this is by plotting a ratio of residual difference optical density for LA and DA samples at wavelengths where neither the reactants nor the ground state

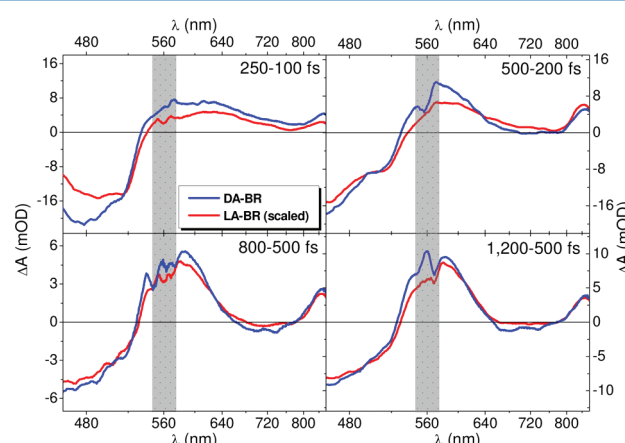


**Figure 4.** Four representative dynamic difference spectra ( $[\Delta\text{OD}(t + \delta t) - \Delta\text{OD}(t)]$ , relevant delay times presented within the panels) for DA-BR (blue lines) and LA-BR (red lines), with the latter multiplied by a constant factor for all delays. This demonstrates that beyond  $\sim 0.5$  ps they overlap perfectly throughout the probed spectral range.

photoproducts absorb. Possibilities are the intense “blue” excited state absorption band or the emission in the NIR. Figure 5 demonstrates that both of these ratios level off near  $0.65 \pm 0.05$  at delays beyond  $\sim 200$  fs, in agreement with all stated assumptions and with the scaling factor used in Figure 4. This ratio can then be used to subtract the  $\text{BR}_{\text{AT}}$  contributions from the DA spectral data, allowing the extraction of the more elusive contributions of the pure 13-cis protein spectra. The right panel in Figure 2, from which the spectral cuts are depicted in Figure 3 using green lines, results from performing the data subtraction with that ratio. From the time dependence displayed in both, we conclude that the IC in  $\text{BR}_{13\text{C}}$  is at least 3-fold faster than in  $\text{BR}_{\text{AT}}$ . Taking into account the temporal

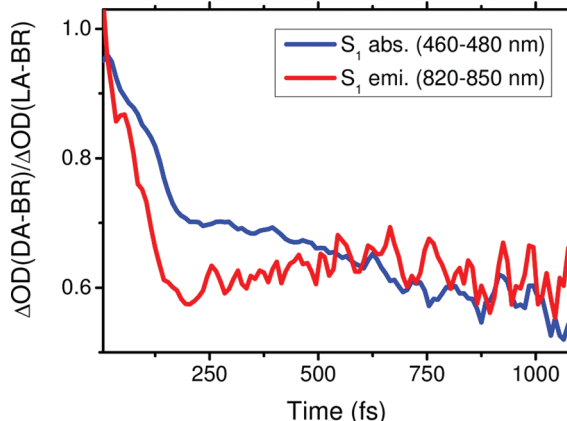
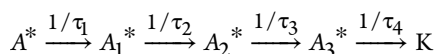


**Figure 5.**  $[\Delta OD_{DA\text{-}BR}(t)/\Delta OD_{LA\text{-}BR}(t)]$  in the  $S_1$  absorption band (460–480 nm) and emission band (820–850 nm), showing an initial  $\sim 200$  fs stage of rapid evolution, assigned to the rapid dynamics due to IC of  $BR_{13C}$ , found only in the DA-BR sample. The curves reach a plateau at delays beyond  $\sim 200$  fs, demonstrating that beyond this point the contributions for the signals of both samples (DA and LA) are due to exclusively  $BR_{AT}$ .

resolution of the experiment and the already rapid IC rate in  $BR_{AT}$ ; this factor is only a lower limit.

To further quantify the spectral evolution, global fitting was conducted with the following sequential kinetic scheme



yielding Evolution Associated Difference Spectra (EADS) and matching decay times shown in Figure 6. The fitting routine also accounts for the finite experimental temporal resolution by convolution with a Gaussian instrument response function of  $\sim 80$  fs fwhm. In view of the high time resolution of current experiments, six distinct species, including the asymptotic photoproduct and a delta-function component representing coherent coupling of pump and probe, were found necessary for high-quality fitting to the data.<sup>56</sup> The initial rapid phase of rearrangement, the rate of IC, and the decay time from J to K obtained by global fitting all agree reasonably with previous pump–probe data studies of  $BR_{AT}$ .<sup>9,10,15,16</sup> In particular, in a recent study of native  $BR_{AT}$ , Briand et al.<sup>26</sup> present decay times in excellent correspondence to our  $\tau_2$ – $\tau_5$ , including the previously unreported  $\sim 1$  ps component.

The EADS components of DA-ASR and LA-ASR seem similar, with mild spectral shifts, but the lifetimes associated with the former are shorter throughout all stages of evolution. The EADS extracted for  $BR_{13C}$ , however, already differ significantly from the other two, in both spectral features and lifetimes. It has two ultrarapid ( $<200$  fs) spectral steps, after which the formation of the K photoproduct and its cooling are apparent. The K intermediate difference spectrum is different even qualitatively, having almost balanced absorptive and emissive lobes in the case of  $BR_{AT}$  and a much more dominant absorptive feature in  $BR_{13C}$ . All of these characteristics are in agreement with the findings of the ASR<sub>AT</sub> vs ASR<sub>13C</sub> study<sup>56</sup> and can be related with the general trend of increasing dipole strength for absorption going from 13-*cis* to all-*trans* due to extended conjugation in the latter. Thus, the observation of significantly enhanced rates of IC in  $BR_{13C}$ , rates that are almost similar to those measured in visual pigments, proves to be

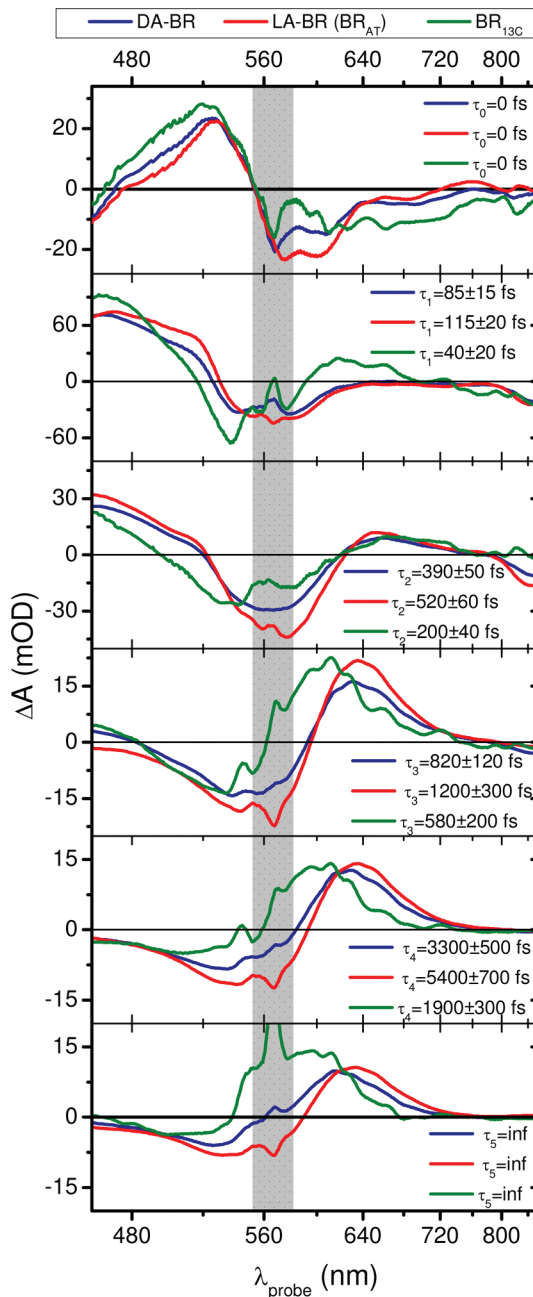


**Figure 6.** Evolutionary Associated Decay Spectra (EADS) derived by global fitting to the sequential kinetic scheme above. The  $BR_{13C}$  EADS were extracted by global fitting of the normalized properly weighted subtraction of LA-BR from DA-BR data sets (see right panel of Figure 2).

robust and fully quantified by the global kinetic analysis presented.

## DISCUSSION

This comparative study, inspired by recent ultrafast measurements on photoswitching in the *Anabaena* Sensory Rhodopsin (ASR),<sup>56</sup> was aimed at recording photochemical dynamics in  $BR_{AT}$  and  $BR_{13C}$ . BR and ASR are both MRPs with stable all-*trans* and 13-*cis* ground state forms, whose relative abundance can be shifted by illumination, without any additional tampering or modification of the protein environment. Despite their mechanistic differences, in both proteins the time scale of

internal conversion is shown to be much faster when initiated in the 13-*cis* ground state. This is demonstrated most clearly in the two panels of Figure 7, presenting scans averaged over the

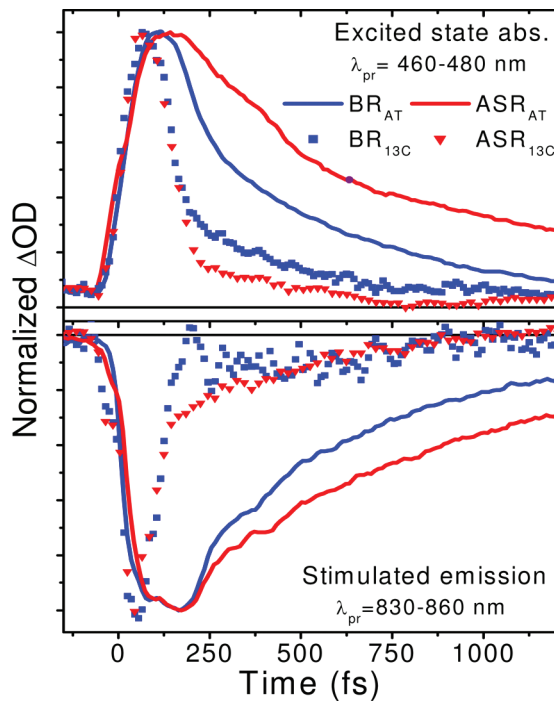


**Figure 7.** Short time excited state absorption and stimulated emission changes, extracted by averaging of the pump–probe data in the designated spectral ranges, for BR<sub>AT</sub>, BR<sub>13C</sub>, ASR<sub>AT</sub>, and ASR<sub>13C</sub> (ref 56), all demonstrating shortening of the excited state lifetimes of the 13-*cis* configurations. See text for details.

peaks of excited state absorption and emission near 470 and 840 nm, respectively, for both proteins. Decay of both excited state measures for the 13-*cis* configuration borders on our experimental time resolution, while the photoexcited all-*trans* proteins emit, and absorb, well beyond a picosecond, indicating shortening factors of excited state lifetimes by more than 3 and 10 for BR and ASR, respectively. This finding is the focus of the discussion below.

It is worthwhile to consider the confidence that these findings warrant, before dealing with their significance. The time resolution of the pump–probe experiments, determined by our cross-correlation to be between 70 and 90 fs, is on the same order of magnitude as the shortest decay components detected, questioning the correctness of their assignments. It is therefore instructive to look back at the spectral cuts presented in Figure 3, particularly the first and the last. As in the case of the ASR protein (Figure 3 in ref 56), no analysis is required to see that transition from an exclusively all-*trans* sample to one mixed with 13-*cis* has caused observable changes in the decay trends, indicating at all four wavelengths a contribution from shorter lived species in the latter. Furthermore, in both proteins, components of 13-*cis* contributions to the data appear which are well within the range which can be separated in time by our methods. Thus, while the fastest time constants extracted by global fitting may not be determined with great precision, the qualitatively discernible trends, and their consistency in both systems, build a convincing argument in favor of the analysis promoted and of the general conclusions

concerning the effects of the initial retinal configuration on the course of IC.

In this respect, we comment also on reference to “rates” of IC in this manuscript. Mention of a rate implies a first-order decay scenario. We have used this term loosely, inferring a shortening or lengthening in the average duration of excited state populations. In reality, the cuts depicted in Figure 3, and in particular the last pertaining to stimulated emission, exhibit temporal structure for all-*trans* reactants, such as delayed rise, sluggish buildup of decay, and low-frequency oscillations, before the later stages for which a kinetic description is more befitting. In native BR<sub>AT</sub>, experiment and theory alike indicate that upon photoexcitation relaxation along the carbon–carbon bond order alternation coordinate precedes an initial breaking of the planar geometry by torsion, which is essential for funneling energy into the reactive torsions.<sup>13,14,20,22,61–64</sup> This initial stage of structural evolution, with possible contributions of the slower motions (such as torsions), may be responsible for the delayed onset of decay so clearly observable in BR<sub>AT</sub> (and also in ASR<sub>AT</sub> in the previous study). These signatures demonstrate that the initial retinal conformation has much more intricate consequences, which once properly assigned through simulation may provide multidimensional structural details of the onset of IC in the different reactant variants.

Previous ultrafast studies of BR have been interpreted in terms of envisioned excited state topologies coined two-state,<sup>65</sup> two-state inertial,<sup>66</sup> two-state two-mode,<sup>61,67</sup> or three-state models.<sup>17,22,68</sup> For the latter, a small potential barrier—resulting from coupling and avoided crossing of two excited state potentials—was suggested for the AT → 13C direction.<sup>13,17,22,25,54,69–72</sup> The existence of such a barrier can also explain the multiexponential dynamics and the stable emission spectrum and cross section during IC,<sup>17,70,73</sup> and it is experimentally supported by temperature-dependence fluorescence studies of BR.<sup>74,75</sup> The observed wavelength independence of photoisomerization quantum yields in BR<sup>76</sup> is also in line with this scenario. Moreover, in a recent QM/MM study of ASR, the reaction coordinate for photoisomerization was mapped, suggesting a small barrier to isomerization exclusively in the AT → 13C direction.<sup>77</sup> To substantiate these models, reactive potential topologies have been addressed by high level quantum chemical simulations,<sup>73,78–81</sup> focusing on reconstruction of a multidimensional reaction coordinate leading from the Franck–Condon state to conical intersections to the ground state. One noticeable difference between the two isomers was observed by molecular dynamics simulations, which proposed that following the photoisomerization of the 13-*cis*,15-*syn* isomer the Schiff base nitrogen points to the intracellular rather than to the extracellular protein site, as opposed to the all-*trans* isomer.<sup>82</sup> However, while simulations have provided insights into how the protein and its embedded water molecules confer bond selectivity and rate enhancement to the stage of isomerization, a comprehensive coverage of these insights is beyond the scope of this discussion. Suffice it to say that the conclusions drawn from theoretical modeling of BR photo-physics do not provide clear predictions of the harsh asymmetry in IC dynamics between BR<sub>AT</sub> and BR<sub>13C</sub> discovered in our experiments.

In terms of experimental study of BR and related molecular systems, a thorough coverage of the literature provides little indication that the initial configuration of the retinal prosthetic group should have such a drastic effect on the course of IC. In solution, excitation of all-*trans* or 13-*cis* RPSB leads to

biexponential decay with similar picosecond rates.<sup>69</sup> While the 13-*cis* isomer used in that study was predominantly 13-*cis*,15-*anti* and not the 15-*syn* isomer, this has been separately shown to have only minor effects on IC kinetics of the all-*trans* isomer.<sup>83</sup> The extreme shortening of IC observed in the 13-*cis* proteins must be, therefore, due to specific protein catalysis. In cases where sequence modifications or environmental manipulation of BR samples has led to coexistence of both isomers in the ground state, the reported effects on IC rates have gone either way—i.e., enhanced IC catalysis of BR<sub>AT</sub> in some cases and of BR<sub>13C</sub> in others.<sup>26,52,53,55,82,84</sup> Furthermore, the IC components discussed were all picoseconds in duration, never suggesting the extreme hastening observed here on a subpicosecond time scale. Finally, as mentioned in the Introduction, the only previous ultrafast spectroscopic experiment on LA-BR and DA-BR reported no difference at all in the duration of IC within their uncertainty.<sup>8</sup>

Input from experiments on BR or ASR, relevant to our dilemma here, may come from resonance Raman, FTIR, NMR, and X-ray crystallography of BR and also of ASR, for both ground state retinal forms. To assess this, we review similar structural and spectroscopic studies pertaining to the visual pigment, where ballistic IC is now well-established. Prestraining of retinal within the rhodopsin pocket, including backbone bending and twisting—quantified by various structure-determining methods—has repeatedly been implicated in the ballistic and nuclear-coherent IC of the rhodopsin,<sup>35,37–39</sup> due either to geometrical constraints<sup>40</sup> or to protein “guidance”.<sup>41,42,85</sup> Theoretical simulations of a similarly twisted 11-*cis* RPSB molecule in the gas phase also support <100 fs evolution toward the CI,<sup>38,40,86</sup> leading to speculation that protein catalysis in rhodopsin is induced solely by determining the initial geometry of the retinal chromophore.<sup>40</sup> Either way, specific interactions with the protein obviously deform the retinal chromophore and should therefore be looked for in the case of the 13-*cis* isomers here as well, following the same rationale.

Structural data on the isomers of BR show that they are both relatively planar and show no signs of protein-induced crowding akin to the visual pigments.<sup>82,87</sup> In addition, both share similar protein structure and matching water-containing hydrogen-bonding networks around the Schiff base,<sup>44</sup> which is also consistent with pressure-dependence reports of the isomeric composition of DA-BR.<sup>88</sup> Mild indications for distortion of the retinal from planarity in the case of 13-*cis* BR were reported in both NMR and resonance Raman studies.<sup>18,89–91</sup> These distortions seem to be negligible when compared to the distortion observed in the case of the 11-*cis* retinal in the visual pigment. However, a close inspection of the X-ray data of DA-BR does point at significant twisting of the C<sub>14</sub>–C<sub>15</sub> single bond, not observed in the case of LA-BR.<sup>44</sup> Theoretical studies of RH and a small model system showed that a twist in a single bond neighboring the isomerizing double bond might induce a spring-like effect, giving additional impetus for isomerization of the latter (here, C<sub>13</sub>=C<sub>14</sub>) and therefore hastening the IC rate.<sup>32,85</sup>

In lieu of hard evidence for drastic differences in initial structure or prestraining, we turn to difference-FTIR spectroscopic studies of BR<sup>92</sup> and of ASR<sup>58</sup> to look for the causes of the vast dynamic differences observed in both experiments. Comparison of cryogenic FTIR for the AT and 13C isomers of both proteins show that: (a) smaller rotational motion of the Schiff base is observed during retinal isomer-

ization in the case of 13-*cis* isomers, (b) widely distributed structural change is apparent upon creation of the K photoproduct in the 13-*cis* vs localized changes near the Schiff base detected for the all-*trans* isomers, and (c) stronger disruption of hydrogen bonds to the Schiff base takes place during K formation in the case of the all-*trans* isomer. The latter finding might account for a potential barrier en route to photoisomerization, which is specific only to the all-*trans* → 13-*cis* direction, already mentioned earlier in the discussion. One should remember, however, that the rates of IC are related to the evolution from the Franck–Condon geometry toward the CI to the ground state, which are not directly comparable to the observed structural differences of the reactant and the K ground state photoproduct.

## CONCLUDING REMARKS

Primary events in light-adapted and dark-adapted BR have been studied anew with high time resolution and continuous hyperspectral coverage throughout the visible into the near IR. Kinetic analysis of the results demonstrates that contrary to earlier claims 13-*cis* BR undergoes internal conversion at least 3 times faster than the biologically active all-*trans* form. Along with similar findings in a recent study of the ASR protein,<sup>56</sup> this may be a general feature of microbial retinal protein photochemistry. A comprehensive survey of the literature pertaining to this issue has produced no clear indication why a vast difference in photoinduced dynamics between the two forms should exist. In particular, none of the mechanisms allegedly responsible for equally rapid internal conversion in the visual pigment rhodopsin, initiated by absorption in an 11-*cis* retinal chromophore, appear to be relevant to the case at hand. Further experimental as well as theoretical investigation will be required to answer this new riddle, which challenges current understanding of protein catalysis of internal conversion in retinal proteins.

## AUTHOR INFORMATION

### Corresponding Author

\*E-mail: sandy@fh.huji.ac.il. Tel.: +972-2-6585326. Fax: +972-2-5618033.

### Notes

The authors declare no competing financial interest.

## ACKNOWLEDGMENTS

We thank Prof. Marco Garavelli for assistance in the review of literature X-ray structures, and interpretation of their dynamic significance. This work was supported by the Israel Science Foundation (ISF), which is administered by the Israel Academy of Sciences and Humanities, and the US-Israel Binational Science Foundation (BSF). A.W. is supported by the Adams Fellowship Program of the Israel Academy of Sciences and Humanities. M.S. holds the Katzir-Makineni chair in chemistry and is supported by the Kimmelman center for Biomolecular Structure and Assembly. The Farkas Center for Light-Induced Processes is supported by the Minerva-Gesellschaft für die Forschung GmbH, München, Germany.

## REFERENCES

- (1) Oesterhelt, D.; Stoeckenius, W. *Nature New Biol.* **1971**, 233, 149–152.
- (2) Stoeckenius, W.; Lozier, R. H.; Bogomolni, R. A. *Biochim. Biophys. Acta* **1979**, 505, 215–278.

- (3) Scherrer, P.; Mathew, M. K.; Sperling, W.; Stoeckenius, W. *Biochemistry* **1989**, *28*, 829–834.
- (4) Kalisky, O.; Goldschmidt, C. R.; Ottolenghi, M. *Biophys. J.* **1977**, *19*, 185–189.
- (5) Sperling, W.; Carl, P.; Rafferty, C. N.; Dencher, N. A. *Biophys. Struct. Mech.* **1977**, *3*, 79–94.
- (6) Hofrichter, J.; Henry, E. R.; Lozier, R. H. *Biophys. J.* **1989**, *56*, 693–706.
- (7) Roepe, P.; Ahl, P.; Herzfeld, J.; Lugtenburg, J.; Rothschild, K. J. *Biol. Chem.* **1988**, *263*, 5110–5117.
- (8) Petrich, J. W.; Breton, J.; Martin, J. L.; Antonetti, A. *Chem. Phys. Lett.* **1987**, *137*, 369–375.
- (9) Dobler, J.; Zinth, W.; Kaiser, W.; Oesterhelt, D. *Chem. Phys. Lett.* **1988**, *144*, 215–220.
- (10) Mathies, R. A.; Brito Cruz, C. H.; Pollard, W. T.; Shank, C. V. *Science* **1988**, *240*, 777–779.
- (11) Kochendoerfer, G. G.; Mathies, R. A. *Isr. J. Chem.* **1995**, *35*, 211–226.
- (12) Kobayashi, T.; Kim, M.; Taiji, M.; Iwasa, T.; Nakagawa, M.; Tsuda, M. *J. Phys. Chem. B* **1998**, *102*, 272–280.
- (13) Haran, G.; Wynne, K.; Xie, A.; He, Q.; Chance, M.; Hochstrasser, R. M. *Chem. Phys. Lett.* **1996**, *261*, 389–395.
- (14) Haacke, S.; Vinzani, S.; Schenkl, S.; Chergui, M. *ChemPhysChem* **2001**, *2*, 310–315.
- (15) Schmidt, B.; Sobotta, C.; Heinz, B.; Laimgruber, S.; Braun, M.; Gilch, P. *Biochim. Biophys. Acta* **2005**, *1706*, 165–173.
- (16) Haacke, S.; Schenkl, S.; Vinzani, S.; Chergui, M. *Biopolymers* **2002**, *67*, 306–309.
- (17) Gai, F.; Hasson, K.; McDonald, J. C.; Anfinrud, P. A. *Science* **1998**, *279*, 1886–1891.
- (18) Smith, S. O.; Braiman, M. S.; Myers, A. B.; Pardo, J. A.; Courtin, J. M. L.; Winkel, C.; Lugtenburg, J.; Mathies, R. A. *J. Am. Chem. Soc.* **1987**, *109*, 3108–3125.
- (19) Pollard, W. T.; Dexheimer, S. L.; Wang, Q.; Peteanu, L. A.; Shank, C. V.; Mathies, R. A. *J. Phys. Chem.* **1992**, *96*, 6147–6158.
- (20) Song, L.; El-Sayed, M. A. *J. Am. Chem. Soc.* **1998**, *120*, 8889–8890.
- (21) Atkinson, G. H.; Ujj, L.; Zhou, Y. *J. Phys. Chem. A* **2000**, *104*, 4130–4139.
- (22) Kobayashi, T.; Saito, T.; Ohtani, H. *Nature* **2001**, *414*, 531–534.
- (23) McCamant, D. W.; Kukura, P.; Mathies, R. A. *J. Phys. Chem. B* **2005**, *109*, 10449–10457.
- (24) Shim, S.; Dasgupta, J.; Mathies, R. A. *J. Am. Chem. Soc.* **2009**, *131*, 7592–7597.
- (25) Ruhman, S.; Hou, B.; Friedman, N.; Ottolenghi, M.; Sheves, M. *J. Am. Chem. Soc.* **2002**, *124*, 8854–8858.
- (26) Briand, J.; Léonard, J.; Haacke, S. *J. Opt.* **2010**, *12*, 084004.
- (27) Diller, R. In *Ultrashort Laser Pulses in Biology and Medicine*; Braun, M., Gilch, P., Zinth, W., Eds.; Springer: Berlin Heidelberg, 2008; pp 243–277.
- (28) Bismuth, O.; Komm, P.; Friedman, N.; Eliash, T.; Sheves, M.; Ruhman, S. *J. Phys. Chem. B* **2010**, *114*, 3046–3051.
- (29) Schoenlein, R. W.; Peteanu, L. A.; Mathies, R. A.; Shank, C. V. *Science* **1991**, *254*, 412–415.
- (30) Haran, G.; Morlino, E. A.; Matthes, J.; Callender, R. H.; Hochstrasser, R. M. *J. Phys. Chem. A* **1999**, *103*, 2202–2207.
- (31) Wang, Q.; Schoenlein, R. W.; Peteanu, L. A.; Mathies, R. A.; Shank, C. V. *Science* **1994**, *266*, 422–424.
- (32) Polli, D.; Altoè, P.; Weingart, O.; Spillane, K. M.; Manzoni, C.; Brida, D.; Tomasello, G.; Orlandi, G.; Kukura, P.; Mathies, R. A.; Garavelli, M.; Cerullo, G. *Nature* **2010**, *467*, 440–443.
- (33) Lugtenburg, J.; Mathies, R. A.; Griffin, R. G.; Herzfeld, J. *Trends Biochem. Sci.* **1988**, *13*, 388–393.
- (34) Kochendoerfer, G. G.; Verdegem, P. J.; van der Hoef, I.; Lugtenburg, J.; Mathies, R. A. *Biochemistry* **1996**, *35*, 16230–16240.
- (35) Brown, M. F.; Heyn, M. P.; Job, C.; Kim, S.; Moltke, S.; Nakanishi, K.; Nevzorov, A. A.; Struts, A. V.; Salgado, G. F. J.; Wallat, I. *Biochim. Biophys. Acta* **2007**, *1768*, 2979–3000.
- (36) Okada, T.; Sugihara, M.; Bondar, A.-N.; Elstner, M.; Entel, P.; Buss, V. *J. Mol. Biol.* **2004**, *342*, 571–583.
- (37) Sugihara, M.; Hufen, J.; Buss, V. *Biochemistry* **2006**, *45*, 801–810.
- (38) Virshup, A. M.; Punwong, C.; Pogorelov, T. V.; Lindquist, B. A.; Ko, C.; Martinez, T. J. *J. Phys. Chem. B* **2009**, *113*, 3280–3291.
- (39) Gascon, J. A.; Batista, V. S. *Biophys. J.* **2004**, *87*, 2931–2941.
- (40) Weingart, O.; Schapiro, I.; Buss, V. *J. Phys. Chem. B* **2007**, *111*, 3782–3788.
- (41) Hayashi, S.; Tajkhorshid, E.; Schulten, K. *Biophys. J.* **2009**, *96*, 403–416.
- (42) Cembran, A.; González-Luque, R.; Serrano-Andrés, L.; Merchán, M.; Garavelli, M. *Theor. Chem. Acc.* **2007**, *118*, 173–183.
- (43) Moltke, S.; Nevzorov, A. A.; Sakai, N.; Wallat, I.; Job, C.; Nakanishi, K.; Heyn, M. P.; Brown, M. F. *Biochemistry* **1998**, *37*, 11821–11835.
- (44) Nishikawa, T.; Murakami, M.; Kouyama, T. *J. Mol. Biol.* **2005**, *352*, 319–328.
- (45) Schoenlein, R. W.; Peteanu, L. A.; Wang, Q.; Mathies, R. A.; Shank, C. V. *J. Phys. Chem.* **1993**, *97*, 12087–12092.
- (46) Birge, R. R.; Einterz, C. M.; Knapp, H. M.; Murray, L. P. *Biophys. J.* **1988**, *53*, 367–385.
- (47) Polli, D.; Brida, D.; Manzoni, C.; Spillane, K. M.; Garavelli, M.; Kukura, P.; Mathies, R. A.; Cerullo, G. Abstract of papers; In *CLEO:2011 - Laser Applications to Photonic Applications*; Optical Society of America: Baltimore, MD, 2011; OSA Technical Digest (CD), paper JThB42.
- (48) Kukura, P.; McCamant, D. W.; Yoon, S.; Wandschneider, D. B.; Mathies, R. A. *Science* **2005**, *310*, 1006–1009.
- (49) McCamant, D. W. *J. Phys. Chem. B* **2011**, *115*, 9299–9305.
- (50) Schapiro, I.; Ryazantsev, M. N.; Frutos, L. M.; Ferré, N.; Lindh, R.; Olivucci, M. *J. Am. Chem. Soc.* **2011**, *133*, 3354–3364.
- (51) Ye, T.; Gershoren, E.; Friedman, N.; Ottolenghi, M.; Sheves, M.; Ruhman, S. *Chem. Phys. Lett.* **1999**, *314*, 429–434.
- (52) Kobayashi, T.; Terauchi, M.; Kouyama, T.; Yoshizawa, M.; Taiji, M. *Proc. SPIE* **1991**, *1403*, 407–416.
- (53) Song, L.; El-Sayed, M. A.; Lanyi, J. K. *Science* **1993**, *261*, 891–894.
- (54) Logunov, S. L.; El-Sayed, M. A.; Lanyi, J. K. *Biophys. J.* **1996**, *70*, 2875–2881.
- (55) Logunov, S. L.; El-Sayed, M. A.; Lanyi, J. K. *Biophys. J.* **1996**, *71*, 1545–1553.
- (56) Wand, A.; Rozin, R.; Eliash, T.; Jung, K.-H.; Sheves, M.; Ruhman, S. *J. Am. Chem. Soc.* **2011**, *133*, 20922–20932.
- (57) Jung, K.-H.; Trivedi, V. D.; Spudich, J. L. *Mol. Microbiol.* **2003**, *47*, 1513–1522.
- (58) Kawanabe, A.; Kandori, H. *Sensors* **2009**, *9*, 9741–9804.
- (59) Oesterhelt, D.; Stoeckenius, W. In *Biomembranes Part A*; Sidney Fleischer, L. P., Ed.; Academic Press: New York, 1974; Vol. 31, pp 667–678.
- (60) Polli, D.; Brida, D.; Mukamel, S.; Lanzani, G.; Cerullo, G. *Phys. Rev. A* **2010**, *82*, 053809.
- (61) Gonzalez-Luque, R.; Garavelli, M.; Bernardi, F.; Merchán, M.; Robb, M. A.; Olivucci, M. *Proc. Natl. Acad. Sci. U.S.A.* **2000**, *97*, 9379–9384.
- (62) Garavelli, M.; Bernardi, F.; Olivucci, M.; Vreven, T.; Klein, S.; Celani, P.; Robb, M. A. *Faraday Discuss.* **1998**, *110*, 51–70.
- (63) Ben-Nun, M.; Molnar, F.; Schulten, K.; Martinez, T. J. *Proc. Natl. Acad. Sci. U.S.A.* **2002**, *99*, 1769–1773.
- (64) Kraack, J. P.; Buckup, T.; Hampp, N.; Motzkus, M. *ChemPhysChem* **2011**, *12*, 1851–1859.
- (65) Rosenfeld, T.; Honig, B.; Ottolenghi, M.; Hurley, J.; Ebrey, T. G. *Pure Appl. Chem.* **1977**, *49*, 341–351.
- (66) Birge, R. R. *Biochim. Biophys. Acta, Bioenerg.* **1990**, *1016*, 293–327.
- (67) Warshel, A.; Chu, Z. T. *J. Phys. Chem. B* **2001**, *105*, 9857–9871.
- (68) Ben-Nun, M.; Molnar, F.; Lu, H.; Phillips, J. C.; Martinez, T. J.; Schulten, K. *Faraday Discuss.* **1998**, *110*, 447–462.

- (69) Logunov, S. L.; Song, L.; El-Sayed, M. A. *J. Phys. Chem.* **1996**, *100*, 18586–18591.
- (70) Olivucci, M.; Lami, A.; Santoro, F. *Angew. Chem., Int. Ed. Engl.* **2005**, *44*, 5118–5121.
- (71) Cembran, A.; Bernardi, F.; Olivucci, M.; Garavelli, M. *Proc. Natl. Acad. Sci. U.S.A.* **2005**, *102*, 6255–6260.
- (72) Molteni, C.; Frank, I.; Parrinello, M. *J. Am. Chem. Soc.* **1999**, *121*, 12177–12183.
- (73) Hayashi, S.; Tajkhorshid, E.; Schulten, K. *Biophys. J.* **2003**, *85*, 1440–1449.
- (74) Alfano, R. R.; Govindjee, R.; Becher, B.; Ebrey, T. G. *Biophys. J.* **1976**, *16*, 541–545.
- (75) Shapiro, S. L.; Campillo, A. J.; Lewis, A.; Perreault, G. J.; Spoonhower, J. P.; Clayton, R. K.; Stoeckenius, W. *Biophys. J.* **1978**, *23*, 383–393.
- (76) Tittor, J.; Oesterhelt, D. *FEBS Lett.* **1990**, *263*, 269–273.
- (77) Strambi, A.; Durbeej, B.; Ferré, N.; Olivucci, M. *Proc. Natl. Acad. Sci. U.S.A.* **2010**, *107*, 21322–21326.
- (78) Altoè, P.; Cembran, A.; Olivucci, M.; Garavelli, M. *Proc. Natl. Acad. Sci. U.S.A.* **2010**, *107*, 20172–20177.
- (79) Levine, B. G.; Martínez, T. J. *Annu. Rev. Phys. Chem.* **2007**, *58*, 613–634.
- (80) Braun-Sand, S.; Sharma, P. K.; Chu, Z. T.; Pisliakov, A. V.; Warshel, A. *Biochim. Biophys. Acta* **2008**, *1777*, 441–452.
- (81) Humphrey, W.; Lu, H.; Logunov, I.; Werner, H. J.; Schulten, K. *Biophys. J.* **1998**, *75*, 1689–1699.
- (82) Logunov, I.; Humphrey, W.; Schulten, K.; Sheves, M. *Biophys. J.* **1995**, *68*, 1270–1282.
- (83) Zhu, J.; Bismuth, O.; Gdor, I.; Wand, A.; Friedman, N.; Sheves, M.; Ruhman, S. *Chem. Phys. Lett.* **2009**, *479*, 229–233.
- (84) Logunov, S. L.; Masciangioli, T. M.; El-Sayed, M. A. *J. Phys. Chem. B* **1998**, *102*, 8109–8112.
- (85) Tomasello, G.; Olaso-González, G.; Altoè, P.; Stenta, M.; Serrano-Andrés, L.; Merchán, M.; Orlandi, G.; Bottoni, A.; Garavelli, M. *J. Am. Chem. Soc.* **2009**, *131*, 5172–5186.
- (86) Frutos, L. M.; Andrzejów, T.; Santoro, F.; Ferré, N.; Olivucci, M. *Proc. Natl. Acad. Sci. U.S.A.* **2007**, *104*, 7764–7769.
- (87) Tajkhorshid, E.; Baudry, J.; Schulten, K.; Suhai, S. *Biophys. J.* **2000**, *78*, 683–693.
- (88) Bryl, K.; Yoshihara, K. *Eur. Biophys. J.* **2002**, *31*, 539–548.
- (89) Smith, S. O.; Pardo, J. A.; Lugtenburg, J.; Mathies, R. A. *J. Phys. Chem.* **1987**, *91*, 804–819.
- (90) Smith, S. O.; De Groot, H. J. M.; Gebhard, R.; Courtin, J. M. L.; Lugtenburg, J.; Herzfeld, J.; Griffin, R. G. *Biochemistry* **1989**, *28*, 8897–8904.
- (91) De Groot, H. J. M.; Harbison, G. S.; Herzfeld, J.; Griffin, R. G. *Biochemistry* **1989**, *28*, 3346–3353.
- (92) Mizuide, N.; Shibata, M.; Friedman, N.; Sheves, M.; Belenky, M.; Herzfeld, J.; Kandori, H. *Biochemistry* **2006**, *45*, 10674–10681.